academicJournals

Vol. 7(1), pp. 1-12, January, 2016
DOI: 10.5897/JPTAF2015.0122
Article Number: 9824F0256972
ISSN 2360-8560

http://www.academicjournals.org/JPTAF

Journal of Petroleum Technology and Alternative Fuels

Full Length Research Paper

Temperature programme reduction (TPR) studies of cobalt phases in γ-alumina supported cobalt catalysts

Olusola O. James[1]* and Sudip Maity[2]

[1]Chemistry Unit, College of Pure and Applied Sciences, Kwara State University, Malete, P.M.B. 1530, Ilorin, Nigeria.
[2]Liquid Fuels Section, Central Institute of Mining and Fuels Research (Digwadih Campus), PO FRI 828108, Dhanbad, India.

Received 10 November, 2015; Accepted 10 December, 2015

Temperature programmed reduction (TPR) is one of the techniques for obtaining information about phases or bulk species in heterogeneous catalysts. Information from TPR analysis can give insights about phase-support interaction and extent of reduction of the phases at different temperatures. TPR technique is a common tool in the characterisation of cobalt based Fischer-Tropsch (FT) catalysts. However, interpretation of TPR profiles of γ-alumina supported cobalt FT catalysts had been characterised with different views on the nature of phases and reduction processes involved. In this report, we use reduction behaviour of unsupported Co_3O_4 to gain insight for more explicit analysis of TPR profiles of γ-alumina supported Co_3O_4 catalysts. The transition $Co_3O_4 \rightarrow CoO \rightarrow Co$ in γ-alumina supported catalysts prepared with wet impregnation with aqueous cobalt nitrate and calcined at temperatures ≤ 350°C gave reduction peaks at 300 to 350°C. Reduction peaks at 500 to 600°C were due to Co-Al mixed oxide phases; most likely Co_2AlO_4 and probably routes formation of the mixed oxide were also discussed. Consideration of tendency of dissolution of γ-alumina during the impregnation of metal salt is instructive toward achieving higher reducibility of Co_3O_4 in the design of cobalt based Fischer-Tropsch catalysts.

Key words: Temperature programmed reduction (TPR) profile, calcinations, Co_3O_4, γ-Al_2O_3, Fischer-Tropsch catalyst.

INTRODUCTION

Increasing energy demand coupled with the awareness of declining petroleum reserves has motivated renewed research and commercial interest in Fischer–Tropsch synthesis (FTS). Different feedstock options (natural gas, coal and biomass) are being explored to produce liquid hydrocarbons as alternative to petroleum (Kagan et al., 2008; Schulz, 1999; Dry, 2002). Commercial FTS operations are based on iron and cobalt based catalysts. H_2/CO ratio of syngas from natural gas do not required water gas shift step which matches the low water-gas shift (WGS) activity of cobalt based catalysts. Moreover, Co-based catalysts are selective towards paraffins and have higher activity for hydrocarbon formation than Fe-based catalysts; hence, cobalt catalysts are preferred for

*Corresponding author. E-mail: sharafeldin99@yahoo.com.

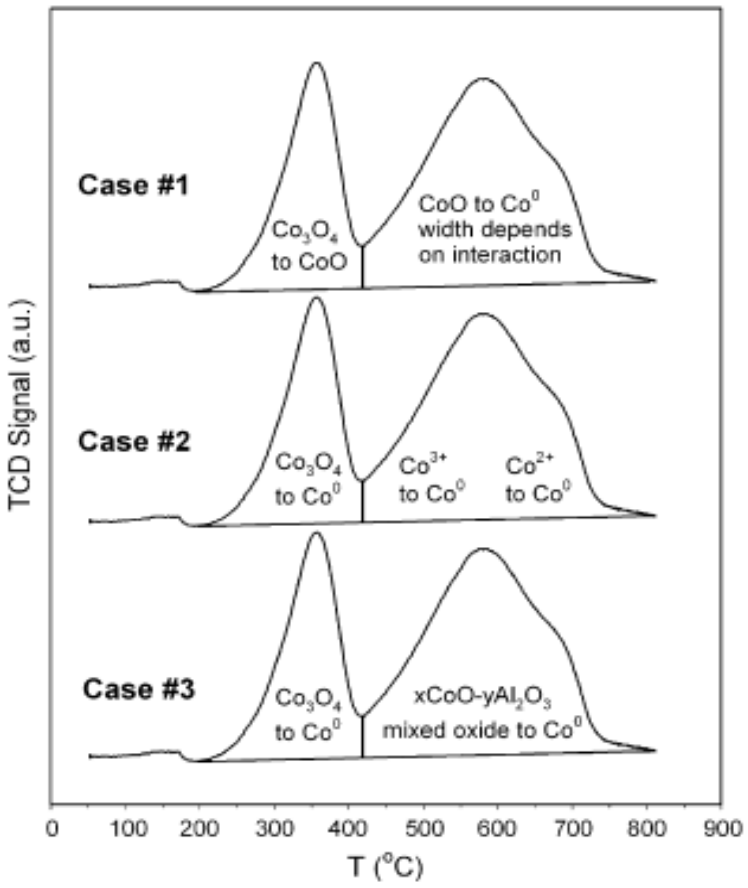

Figure 1. Case scenarios in the interpretation of observed peaks in standard H-TPR patterns for Co/Al_2O_3 catalysts (Jacobs et al., 2007).

gas-to-liquid (GTL) projects (Perego, 2007; Schulz, 1999; Schulz, 2003).

Active sites in cobalt based catalysts are cobalt metal nanoparticles and several studies have shown positive correlations between cobalt dispersion and FTS activity and hydrocarbon selectivity (Iglesia, 1997; Girardon et al., 2007). Thus, maximizing cobalt dispersion on the support is a key objective in the design of Co-based catalysts (Khodakov, 2009). Generally, preparations of cobalt catalysts involve impregnation of high surface area support material with cobalt salt solution, followed by drying and calcination. During calcination, the impregnated salt is transformed into oxide phase(s). The active phase for the FT synthesis are generated *in situ* by reduction under hydrogen stream prior to passage of syngas feed (Zhang et al., 2002; Sirijaruphan et al., 2003).

Gamma (γ) alumina is often a prefer support for cobalt catalysts because of its ability to stabilize small size clusters of cobalt particles and high resistance to attrition especially in the continuously stirred tank reactor or slurry bubble column reactor. However, several reports have advanced that after activation, considerably large fraction of the impregnated cobalt precursor on γ-alumina are catalytically inactive for the hydrocarbon synthesis (Chu et al., 2007; Sirijaruphan et al., 2003). An important of objective in the design of cobalt-based Fischer-Tropsch synthesis is to maximise the proportion of impregnated cobalt precursor on γ-alumina that become reduced to the metallic phase. Temperature programmed reduction (TPR) technique is useful barometric tool for studying the reduction behaviour of catalysts. However, there are varied interpretations of H-TPR profiles of γ-alumina supported FTS cobalt catalysts. These interpretations was categorised and summarised by Jacobs et al., (2007) (Figure 1). Case 1 scenario is the most popular, with the view that the predominant phase of the cobalt is as Co_3O_4 and it undergo reduction to metallic cobalt in a two stage process: $Co_3O_4 \rightarrow CoO \rightarrow Co$, at temperatures ranges 200 to 400°C and 400 to 800°C, respectively. Case 2 and Case 3 scenarios recognised Co_3O_4 phase with a one-stage reduction to Co, at the temperature ~ 300 to 350°C. The advocates of the Case 2 and Case 3 viewpoints believed that γ-alumina supported FTS cobalt

Table 1. Sample preparation parameters.

Sample ID	Calcination condition	
	Temp (^oC)	Duration (h)
Unsupported Co_3O_4		
A	185	8
B	200	6
C	250	6
D	350	6
γ-alumina-supported Co_3O_4		
E	110	12
F	150	8
G	185	8
H	200	6
I	250	6
J	350	6

catalysts also contain CoO or $xCoO\text{-}yAl_2O_3$ cobalt phases. It is argued that reduction of these phases account for H-TPR peaks in the temperature range of 400 to 800°C. The three proposals recognised the possibility of cobalt-aluminate phase which is reduced above 800°C. While there is yet a consensus on reduction behaviour of alumina supported cobalt catalyst, the aforementioned highlighted perspectives in the interpretations of H-TPR profiles have influenced approaches to design of alumina supported cobalt based FT catalysts. This study is motivated by the need for correct interpretations of H-TPR profiles alumina supported cobalt catalysts that are intended for Fischer-Tropsch application. Hence, we present results of H-TPR studies of unsupported cobalt oxide as reference to gain insight about reduction behaviour of γ-alumina cobalt catalysts. X-ray diffraction (XRD) was also used to identify the Co-oxide phases and determine their crystallite sizes. Reducibility of the supported catalysts was determined by O_2-titration. Estimates of percentage reduction of the catalysts were also made from the TPR profiles. Result of this study does not agree with two stage process (Case 1; $Co_3O_4 \rightarrow CoO \rightarrow Co$) for conversion of cobalt oxide to metallic cobalt. It shows that design of alumina supported cobalt catalysts should be approached with the view of cobalt oxide reduction following the Case 3 scenario.

METHODOLOGY

Catalyst preparation

Unsupported Co_3O_4 samples were prepared by calcining cobalt nitrate hexahydrate [$Co(NO_3)_2.6H_2O$, Merck, India] at 185, 200, 250 and 350°C for 8, 6, 6 and 6 h, respectively. Gravimetric measurements of their thermal decomposition in static air were carried out by weighing 5 g of the salt into pre-weighed clean alumina crucibles. After calcination, the crucible and the contents were cooled in a desiccator, re-weighed and the mass loss recorded. Single lot of 60 g of supported cobalt catalyst is prepared by wet impregnation method with cobalt loading (20 mol %) on γ-alumina (Sasol GmbH, Germany, Extrudates, 1.6/200, Lot: E317, Spec.: 665100, bulk density 0.73 g/cm^3; BET Surface Area 181 m^{2}g^{-1}; Pore Volume: 0.49 cm^{3}g^{-1}). The sample was dried for 12 h at 110°C and divided into six equal portions. Details of calcination of the catalysts are presented in Table 1.

X-ray diffraction

XRD patterns were recorded at room temperature on a D8 ADVANCE (BRUKER AXS, Germany) diffractometer using CuK_α radiation with parallel beam (Gobel Mirror). The catalysts were ground to fine powder prior to measurement. The scans were recorded in the 2θ range between 10 and 75° using step size of 0.02° and scan speed of 2 s/step. Peaks were identified by search match technique using DIFFRAC^{plus} software (BRUKER AXS, Germany) with reference to the JCPDS database. The software TOPAS 3.0 from Bruker AXS (2005) was used for refinement of Co_3O_4 diffraction peak (311) located at 2θ = 36.9° to determine the average crystallite size.

Temperature programmed reduction (TPR)

TPR profiles of the samples were recorded with ChemiSorb 2720 (M/s Micrometrics, USA) equipped with a TCD detector. The TPR profiles were obtained by reducing the catalyst samples by a gas mixture of 10% H_2 in Ar with a flow rate of 20 ml/min while the temperature was increased from ambient to 800°C at a rate of 10°C/min.

Reducibility

Reducibility of the supported catalysts was determined by *O_2-titration* which was designated by R_o and calculation of which was expressed by the Equation - 1. The catalysts were first reduced at 350°C for 8 h with pure hydrogen and re-oxidised with 5% O_2 in Helium gas at the same temperature using pulse chemisorption technique. The percentage of R_o was calculated by assuming complete re-oxidation of Co to Co_3O_4 according to the chemical equation: $3Co + 2O_2 \rightarrow Co_3O_4$.

$$\%\, R_O = \frac{no\ of\ mole\ of\ O_2\ uptake}{stochiometric\ no\ of\ mole\ of\ O_2} \times \frac{3}{2} \times 100 \quad -- \quad (1)$$

Reducibility determined by TPR technique is expressed as R_H and calculated according to equation 2. Complete reduction of Co_3O_4 phase was assumed and the TPR profile was deconvoluted to corresponding peak areas. The deconvolution of the TPR signal was made with the ChemiSoft software package provided by M/s Micrometrics, USA. The peak temperature was fixed for the deconvolution of the TPR profiles.

$$\%\, R_H = \frac{area\ of\ \beta\ peak}{sum\ of\ area\ of\ \alpha, \beta, \gamma\ peaks} \quad ---- \quad (2)$$

α, β and γ are the reduction peaks assigned to nitrate, Co_3O_4 and cobalt-aluminate in the resolved TPR profiles of the supported catalysts**.**

Table 2. Gravimetric results of thermal decomposition of cobalt nitrate in static air at different temperatures.

Samples (°C)	% Δm (Cal. – Expl)	
	Co_2O_3	Co_3O_4
A (185)	0.57	1.48
B (200)	0.04	0.95
C (250)	-0.31	0.61
D (350)	-0.42	0.49

RESULTS AND DISCUSSION

Gravimetric measurements of thermal decomposition

It has been reported that thermal decomposition of cobalt nitrate to cobalt oxides (Co_2O_3 and Co_3O_4) in an inert atmosphere starts at 185°C (Ehrhardt et al., 2005). This informed the choice of lowest calcination temperature for unsupported cobalt catalysts for this study. Result of the gravimetric measurements of thermal decomposition of cobalt nitrate in static air is presented in Table 2. Due to possibility presence of residual nitrate due to incomplete decomposition of the nitrate salt we anticipated that the calculated value will be higher than the experimental mass loss. Table 2 showed difference between percentage calculated and experimental mass loss of decomposition of $Co(NO_3)_2.6H_2O$ decreases with increasing calcination temperature.

Positive values are obtained for differences based on decomposition of $Co(NO_3)_2.6H_2O$ to Co_3O_4 at all temperatures. While values obtained based on decomposition of $Co(NO_3)_2.6H_2O$ to Co_2O_3 gave negative values at 250 and 350°C. Since negative different is impracticable, we inferred that Co_3O_4 is the most probable oxide of phase of cobalt after calcination of the supported catalysts. This inference from our hypothesis of presence of residual nitrate agrees with many reports in which Co_3O_4 phase is obtained after calcination of cobalt nitrate. We also obtained peaks assigned to residual nitrate in the H-TPR profile, and hydrogen consumption from those peaks are related to residual nitrate content after calcination of the cobalt salt (*infra verde*). However, report of Ehrhardt et al., (2005) indicated presence of Co_3O_4 and Co_2O_3 phases when cobalt nitrate is calcined in inert atmosphere. Concurrent transformation of the oxides to metallic cobalt takes place in a reducing atmosphere. The oxides are completely reduced to metallic state at temperature less than 400°C. The transformation from cobalt nitrate to metallic cobalt proceeds as follows:

$$Co(NO_3)_2.6H_2O \xrightarrow{35^oC} Co(NO_3)_2.4H_2O \xrightarrow{67^oC} Co(NO_3)_2.2H_2O \xrightarrow{110^oC} Co(NO_3)_2$$

$$Co(NO_3)_2 \xrightarrow{185\text{–}200^oC} \tfrac{m}{5} Co_2O_3 + \tfrac{(1-m)}{5} Co_3O_4 + \tfrac{2}{5} N_2O_4 + \tfrac{3}{5} N_2O_5$$

Where the coefficient '*m'* decreases with the increase of temperature and duration of calcinations.

$$\tfrac{m}{5} Co_2O_3 + \tfrac{(1-m)}{5} Co_3O_4 + \tfrac{7}{5} H_2 \xrightarrow{185-350\,^oC} Co + \tfrac{7}{5} H_2O$$

In the preparation of supported cobalt catalyst, the calcination stage is usually carried out under static or air flow conditions. In these conditions, Co(II) ions can be readily oxidised to Co(III) ions. Moreover, the decomposition of cobalt nitrate produces oxidizing gases, (NO_x), which can aid the oxidation process. This condition should favour formation of Co_2O_3. Prominence of Co_3O_4 phase or rare presence of in characterisation studies of supported cobalt catalysts may be attributed to stabilities of the phases.

Crystallite size

XRD of unsupported and γ-alumina supported catalysts also depict presence of Co_3O_4 phase (Figures 2 and 3). This corroborates the inference from the gravimetric analysis. Crystallite size of the Co_3O_4 of the catalysts calcined at different temperature is presented in Table 3. In both unsupported and γ-alumina supported catalysts crystallites size of Co_3O_4 increases with increase in calcination temperature except the unsupported sample calcined at 185°C which is an outlier. Reason for this outlier situation is not clear at the moment. At the same temperature Co_3O_4 crystallite sizes are smaller in the supported than in unsupported catalysts. This is due to stabilization of Co_3O_4 nanoparticles by the support and in each case the increasing crystallite size with increasing calcination temperature can be attributed to sintering which is promoted at higher temperatures.

H-TPR analysis

Unsupported Co_3O_4 samples

Figure 4 shows the H-TPR profiles of the unsupported Co_3O_4 catalysts. The temperature ranges of the peaks in the profiles are > 200; 270 to 280; 319 to 326 and 375 to 400°C. The peaks are assigned to three transitions presented in Table 4. The first hydrogen consumption temperature range is attributed to reduction of residual nitrate. The second and the third ranges assigned to $Co_3O_4 \rightarrow CoO$; while the fourth is ascribed to $CoO \rightarrow Co$. The profiles display similar trends with those reported by Chen et al., (2003), for CoO_x ($1.00 < x < 1.33$) nanoparticles where it was shown that the value of 'x' influenced pattern of H-TPR profile of CoO_x; x = 1, a single peak was obtained. For x > 1, a shoulder peak developed in the profile of CoO_x samples and was attributed to two stage reduction of the oxides vis - $CoO_x \rightarrow CoO \rightarrow Co$. Increase in the area of the shoulder peak

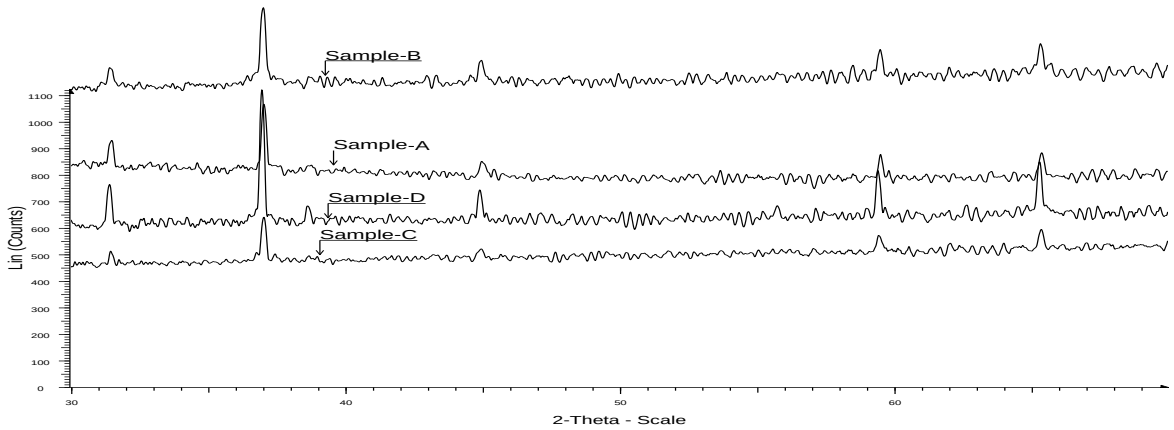

Figure 2. XRD of the unsupported Co_3O_4.

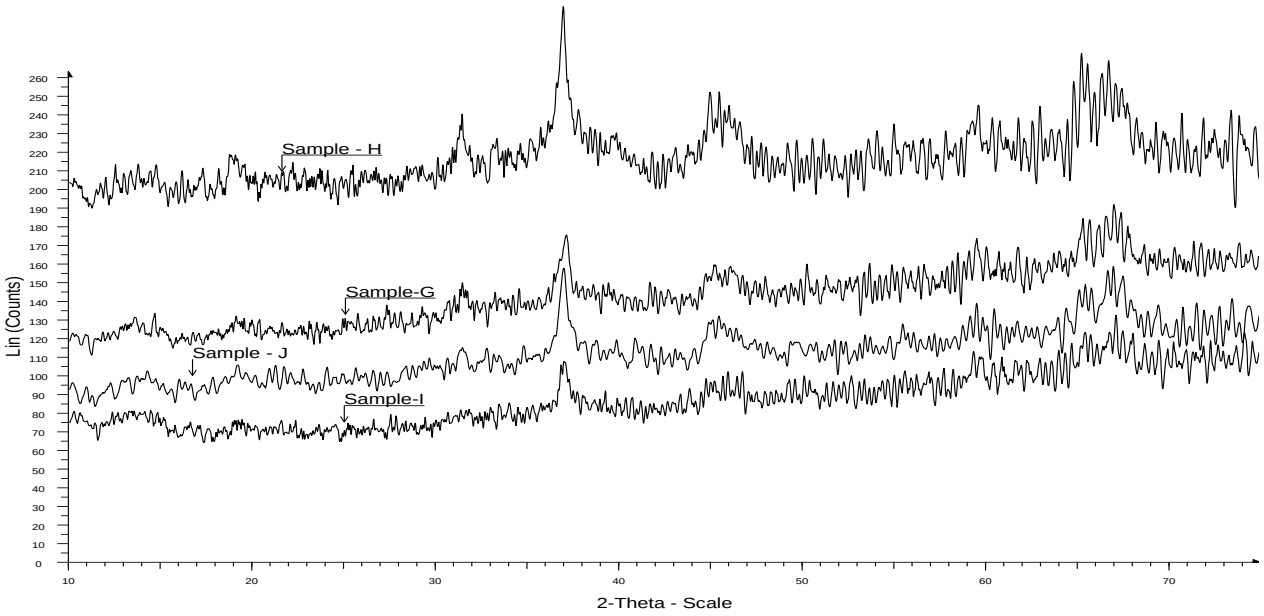

Figure 3. XRD of the γ-alumina supported Co_3O_4.

is proportional with the value of 'x'. They report that the dominant reduction peak temperatures decreased as the values of 'x' increases. The assigned transitions also agree with the report of Yuvaraj et al., (2003). These authors investigated direct reduction of transition metal nitrates with hydrogen. They advanced that reduction of transition metal nitrates is activated by their decomposition and nitrate salts decompose at temperature range between 177 to 270°C. In particular, the temperature ranges 242 ± 30° and 242 ± 20°C was reported for decomposition and reduction of cobalt nitrate, respectively.

The peak temperatures assigned to reduction of residual nitrate decreases with increase in calcination temperature and are similar for catalysts C and D. Peak temperatures attributed to CoO → Co transition increases with the increase of calcination temperature and catalyst B and C also show similar temperature for CoO→ Co reduction. The trend of CoO → Co reduction peak temperature agrees with the report of Tang et al., (2008) in which it was shown that temperature of reduction of CoO_x species increases with the increase of calcination temperature. Potoczna-Petru and Kępiński (2001) also demonstrated that initiation temperature of reduction of Co_3O_4 increases with increase in calcination temperature. With the help selected area electron diffraction (SAED) and high resolution transmission electron microscopy (HRTEM) analyses the authors showed that crystallite

Table 3. Particles size of Co_3O_4 phase in unsupported and γ-alumina supported samples.

Sample ID	Calcinations Temp (°C)	Crystallite size of Co_3O_4 phase (nm)
Unsupported Co_3O_4		
A	185	71.1
B	200	56.5
C	250	62.0
D	350	86.5
γ-alumina-supported Co_3O_4		
E	uncalcined	-
F	150	-
G	185	17.4
H	200	19.8
I	250	22.2
J	350	27.6

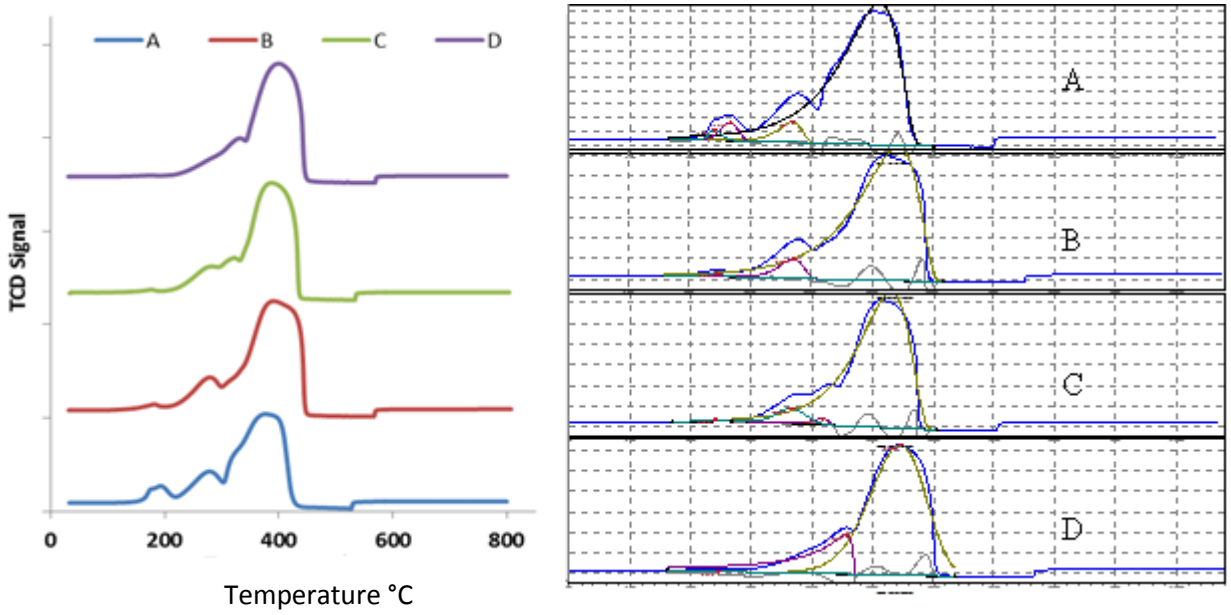

Figure 4. H-TPR profiles of unsupported Co_3O_4 .

size and morphology have strong influence on extent of reduction of Co_3O_4. They also demonstrated that the reduction of Co_3O_4 occurs via preferential epitaxial growth of CoO and Co phases on Co_3O_4 in course of the reduction process. Thus, reduction temperatures presented in Table 4 followed the same trend with similar studies in the literature.

Results in Table 4 indicated that temperature gap between peaks assigned to Co_3O_4 → CoO and CoO → Co reduction stages narrows with increasing temperature. Deconvolution and analysis of the peak areas in the H-TPR profiles of unsupported Co_3O_4 samples show that the percentage residual nitrate decreases with increasing calcination temperature. The areas under the peaks assigned to residual nitrate follow similar trend with the result of the gravimetric analyses (Figure 5). The ratios of the peak area assigned to Co_3O_4 → CoO and CoO → Co, presented in Figure 5, suggest that the ratio varies with calcination temperature. Although the raw profile showed that the shoulders to the main peak (assigned to Co_3O_4 → CoO reduction stage) are more visible in samples calcinated at lower

Table 4. TPR peak temperatures of unsupported Co_3O_4 samples.

Sample ID	Calcination Temperature (°C)	TPR Peak Temperatures (°C)		
		α-(residual nitrate)	β-(Co_3O_4, CoO)	γ- (CoO, Co)
A	185	192	274	376
B	200	182	275	391
C	250	176	272	388
D	350	175	327	400

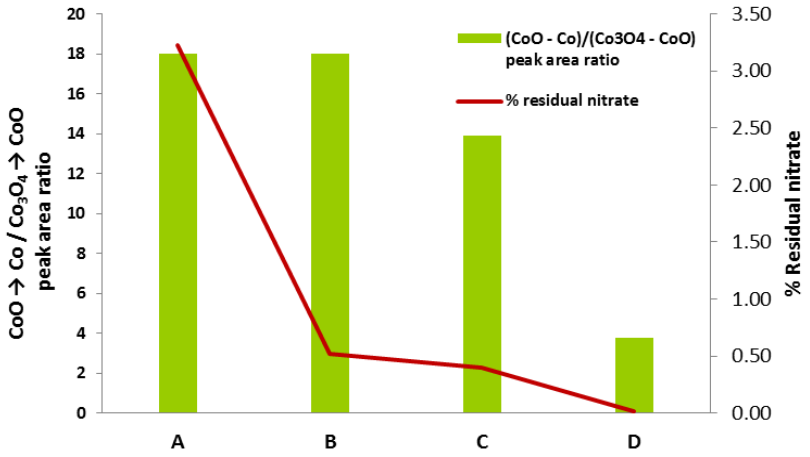

Figure 5. Percentage residual nitrate and CoO → Co / Co_3O_4 → CoO peak area ratio in the unsupported Co_3O_4 samples calcined at different temperatures.

temperatures, the deconvoluted chart indicated that this (Co_3O_4 → CoO) reduction stage is a less distinct stage samples but its signature become more noticeable in the sample calcinated at higher temperatures. Thus, we inferred from the H-TPR profiles that reduction of Co_3O_4 appear to be a two stage reaction, Co_3O_4 → CoO→ Co, with process reduction narrow temperature gap (73 to 126°C). This conclusion corroborates the report of Chen et al., (2003) and Yuvaraj et al., (2003). It also agrees with the report of Wang et al. (2004). They also advanced that reduction of Co_3O_4 to metallic cobalt occurs in two stages at 160 to 230°C (Co_3O_4 → CoO) and 230 to 380°C (CoO → Co). Using *in situ* STG-TPR, these authors showed that reduction of Co_3O_4 and CoO is accompanied by change of shape and crystal structure: Co_3O_4 (hollow spheroidal shape) → face centered cubic (CoO). They added that CoO → Co transition is also associated with changes in the microstructure of the cobalt phases.

Supported Co_3O_4 samples

We attempted interpretation of the reduction pattern of γ-alumina supported cobalt catalysts with the backgrounds from the TPR profiles of unsupported Co_3O_4. Figure 6 shows the TPR profiles of the alumina supported Co_3O_4 samples. The TPR profiles can be deconvoluted into three peaks as presented in Table 5. The first peak (α – peak) is assigned to nitrate reduction. Compared to the unsupported catalysts, these peaks appeared at higher temperatures, which increased with increasing temperature of calcination of the supported catalysts. This may be due to interaction with the surface of the alumina support. Highest peak temperature in the unsupported Co_3O_4 is 400°C, and invoking crystallites effect of highest lower peak temperature of Co_3O_4 phase in the supported catalyst is expected to be below 400°C. However, the profiles of the supported Co_3O_4 contain peaks at temperature above 400°C. Moreover, the temperature gaps between the two higher temperature peaks in supported Co_3O_4 are much wider (191 to 436°C) than in the unsupported samples. Based on these observations we posit that the transitions in the third or γ-peaks of the unsupported and γ-alumina supported cobalt catalysts are different.

Except sample E, the second peaks in the profiles of γ-alumina supported are assigned to Co_3O_4 → Co transition. These peaks are at lower temperatures compared to similar transition in the unsupported counterparts. The lowered Co_3O_4 → Co transition temperature here is attributable to crystallites size effect

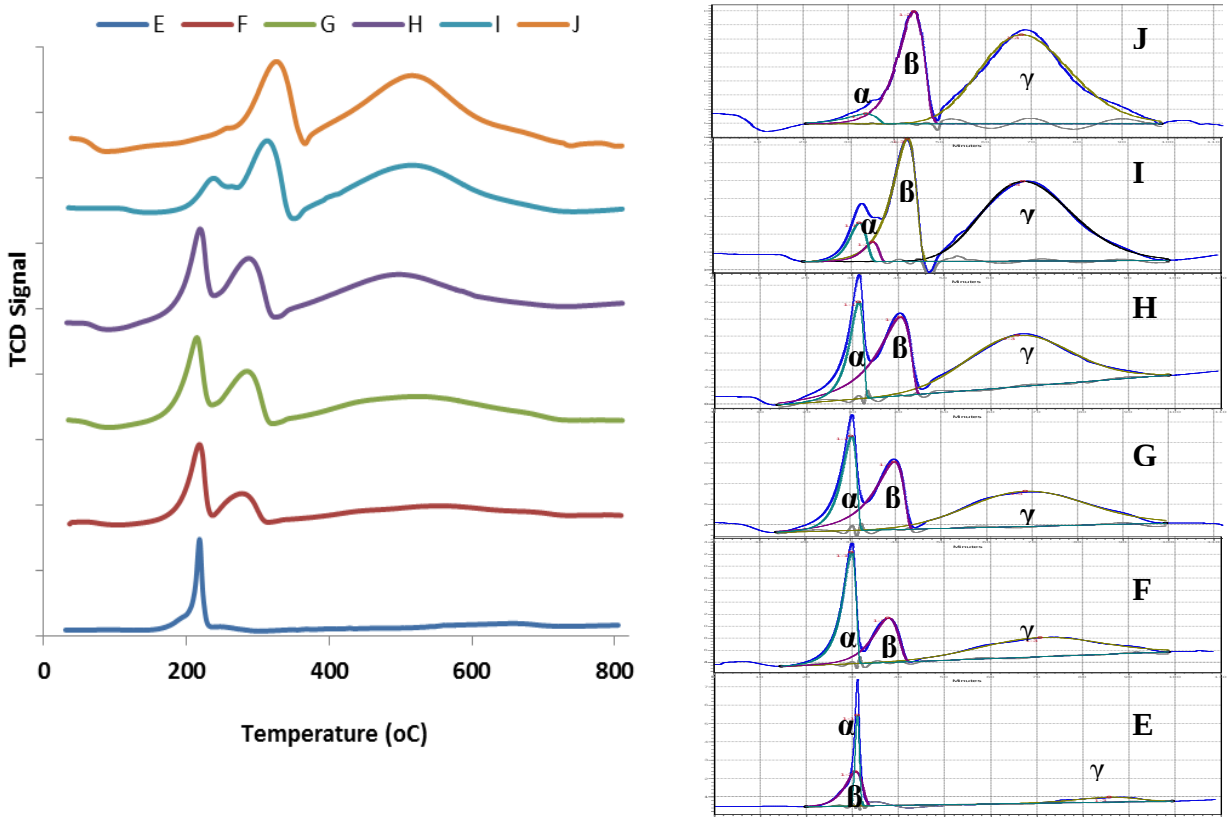

Figure 6. TPR profiles of γ-alumina supported Co_3O_4 catalysts.

Table 5. Peak temperatures of the TPR profiles of the Co/Al_2O_3 samples.

Sample ID	Calcination Temperature (°C)	TPR Peak Temperatures (°C)		
		α	β	γ
J	350	262	326	517
I	250	236	313	517
H	200	219	287	520
G	185	219	285	523
F	150	218	276	542
E	110	218	218	654

in agreement with related literature reports (Potoczna-Petru and Kępiński, 2001; Wang et al., 2004). The prominent peak in the uncalcined catalyst (E) consists of overlap of two peaks: nitrate and $Co_3O_4 \rightarrow Co$ transition peaks. The third peaks (γ – peaks) which range from 517°C (for calcined catalyst) to 654°C (for uncalcined catalyst) are designated to the reduction of cobalt-aluminium mixed oxide. The following trends are observed from the profiles of the supported catalysts: (i) temperature of nitrate (α – peak) increases but peak area decreases with increasing calcination temperature; (ii) temperature and peak area of $Co_3O_4 \rightarrow Co$ (β – peaks) transitions increasing with increasing calcination temperature; (iii) increasing visibility of the third (γ-peaks) with increasing calcination temperature. These third peaks are absent in the unsupported catalyst.

Dispersion and reducibility of supported cobalt catalysts is usually estimated using H_2 chemisorption and O_2 titration technique. Depending on cobalt loading, the reducibility values for unpromoted alumina based catalysts commonly vary between 10 to 45% (Jacobs et al., 2002; Borg et al., 2007). The temperature, 350°C, is

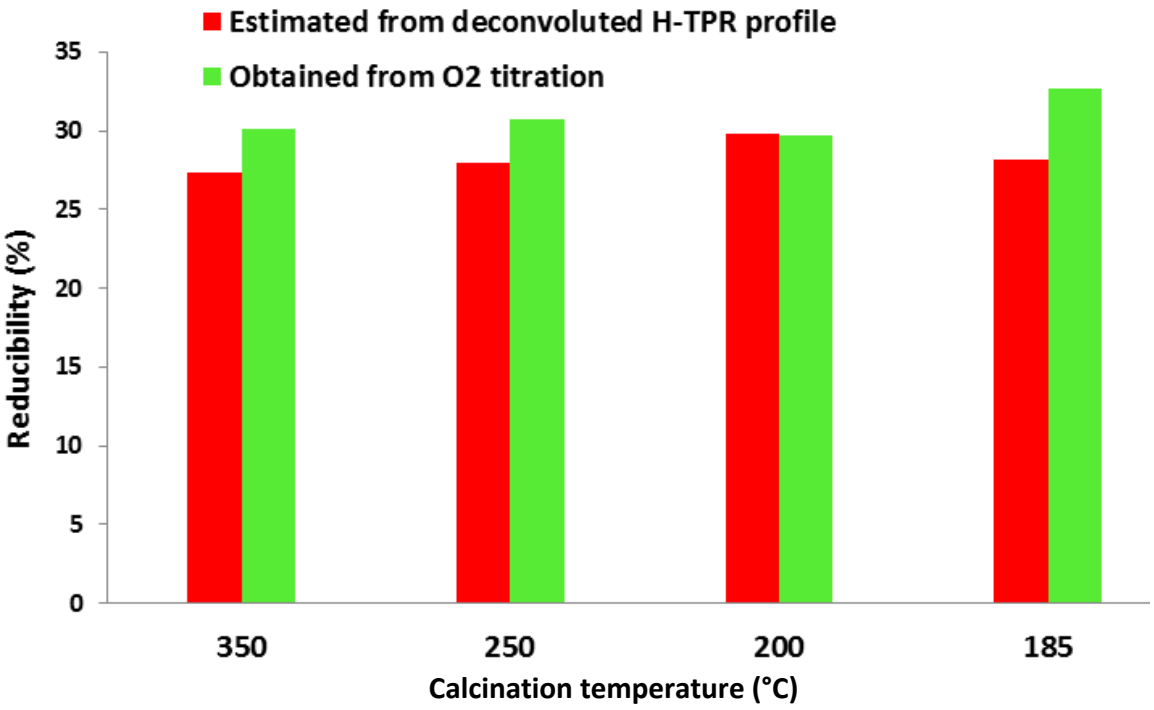

Figure 7. Comparison of Reducibility values from TPR profile estimates and O_2 -titration analysis.

widely adopted as the standard reduction temperature of supported cobalt catalysts for these analyses. This adopted temperature presupposes formation of metallic cobalt phase should take place at ≤ 350°C. It corroborates with the reduction temperatures obtained for unsupported Co_3O_4, and in effect ruled out Case# 1 scenario (Figure 1).

Results of reducibility of the supported Co_3O_4 catalysts are shown in Figure 7. Reducibility values obtained from H-TPR agrees well with values obtained from O_2-titration method. It is observed that the reducibility determined from both the techniques has little variation of values with reference to the increase of calcination temperature. Since residual cobalt nitrate is readily transformed to cobalt during reduction in hydrogen at 350°C, the small difference may be attributed to possibility of metallic cobalt contribution from residual nitrate. The results indicated that calcination temperature has little or no influence on the reducibility of the Co/Al_2O_3 catalysts; crystallite size of Co_3O_4 phase and by extension dispersion of metallic cobalt nanoparticles in reduced catalysts decreases with increasing calcination temperature.

Figure 8 shows the summary of deconvolution analysis of the profiles in Figure 6. The area of the α-peaks decreases expectedly with increasing calcination temperature. It was expected that the areas of α peaks will decreased progressively from catalyst E to J. But F (calcined at 150°C) showed higher percentage hydrogen consumption than catalyst E (calcined at 110°C). According to TGA profiles of cobalt nitrate by Ehrhardt et al., (2005), calcination temperatures of the two catalysts (E and F) are below decomposition of cobalt nitrate, but may contain different amount of hydrated water molecules. The hydrated water molecules contribute to mass of the catalyst and it is expected to be higher in catalyst E than in catalyst F. Thus catalyst F will contain higher amount of cobalt nitrate per unit mass than catalyst E. This may account for the observed higher percentage hydrogen consumption production of nitrate peak of catalyst F compared to catalyst E.

The areas of the β- and γ-peaks increase with increase in calcination temperature. The shape of the Co_3O_4 reduction peak is similar for both the supported and unsupported catalysts, but the signature of two stage reduction of Co_3O_4 particle to Co is not distinguished in the TPR profile of the supported catalysts. Due to smaller crystallite size of Co_3O_4 phase in the supported compared to unsupported catalysts, the two stage reduction process, $Co_3O_4 \rightarrow CoO \rightarrow Co$, are combined in the β peaks. It is worth noting that there is a compromise between nitrate removal and Co_3O_4 crystallite in the supported catalysts. Temperature 250°C appears to be a reasonable compromise between the two ends. The same has also been suggested in the literature as optimum calcination temperature towards achieving higher cobalt dispersion on γ-Al_2O_3 (Borg et al., 2007; Belambe et al., 1997).

Cobalt phase in catalyst E is essentially in the nitrate form. As reported by Yuvaraj et al. (2003), concurrent

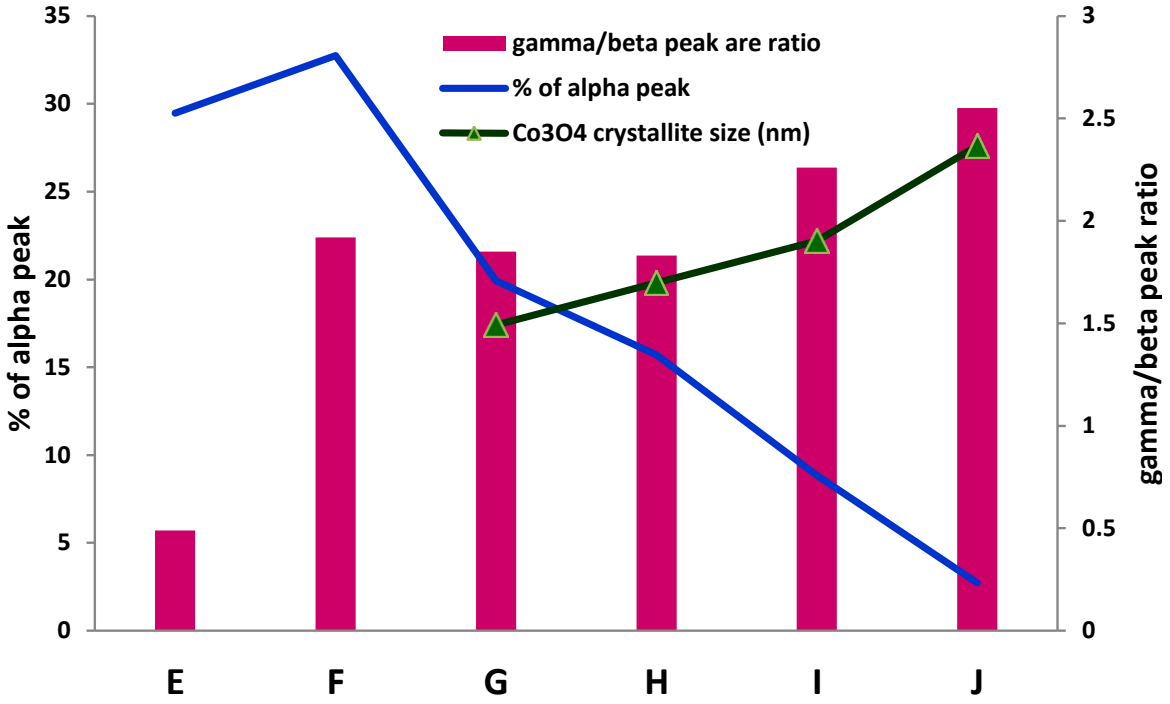

Figure 8. Summary of decomposition analysis of TPR profiles of the supported Co_3O_4.

decomposition and reduction of cobalt nitrate is expected at 242 ± 30°C, thus H-TPR profile of catalyst E ought not to show any peak at temperature above 350°C. However, the profiles of catalyst E showed unexpected hydrogen consumption over a broad temperature range with peak temperature at 650°C. This suggest that prior to calcination the impregnated cobalt nitrate had interacted with γ-alumina supported to form cobalt phases that are not reducible at typical reduction temperature of Co_3O_4 phase. While the scope of the present does not cover identification of this cobalt phase, it is important to draw attention to the point that contrary to the widely held view that γ-alumina is inert in aqueous environment, it has been shown that γ-alumina is active in aqueous media.

Carrier et al., (2007) demonstrated that hydroxide polymorphs of aluminium are thermodynamically more stable phases than γ-alumina in aqueous media. They also showed that γ-alumina transformed to hydroxide polymorphs in aqueous environment. The transformation takes place via surface hydration and dissolution. The dissolution can produce autonomous aluminium hydroxide phase from a supersaturated solution of dissolved aluminium ions. The dissolution process can also be aided by presence of H^+, OH^-or by metal ions (for example, Ni^{2+}, Co^{2+}) (Trueba and Trasatti, 2005). Thus, in effect γ-alumina in contact with aqueous metal ions solution during catalyst preparation via impregnation method has two active phases – surface hydroxide and dissolved Al^{3+}. The surface O-Hs accounts stabilize nano clusters or particles, leading to the widely recognised high dispersion of impregnated metal of metal oxide in γ-alumina support. The second implication of alteration of γ-alumina in aqueous media to catalyst preparation is that, during evaporation stage of impregnation process it leads to supersaturation of dissolved Al^{3+} ions which precipitate as independent hydroxide phase or co-precipitate with metal ions being impregnated on the γ-alumina. Co-precipitation of Al^{3+} ions with divalent metal ions like Co^{2+} can form hydrotalcite-like mixed oxide phase (Ay et al., 2009).

Formation of hydrotalcites-like structures in co-precipitated of Co^{2+} and Al^{3+} ions had been reported by Khassin et al., (2001). They demonstrated that during calcination the hydrotalcites-like structures are transformed into aluminates through inverted spinel-like structure. But at moderate temperatures the hydrotalcites-like structures transformed into Co oxide phase on a highly defective inverted spinel-like structure, in which Co^{2+} enter the support structure and occupy both tetrahedral and octahedral positions. The authors explained that octahedron coordinated Co species are reduced at 580 to 620°C, reduction at 470 to 480°C can also yield Co° supported on inverted spinel-like structure, which contains Co^{2+} in the octahedral coordination. Reduction at 600°C transforms the support to 'ideal' spinel, which contains no octahedron coordinated Co^{2+}. According to Pe et al., (2001), these cobalt phases may yield metallic when reduced in hydrogen at ≥ 480°C.

Thus, we suggest that the cobalt phase responsible for the γ-peaks of catalyst F-J are attributed to hydrotalcite-

like structures, dehydration and dehydroxydecarbonation of these structures appear to at 150 to 200 and 250 to 300°C in air, respectively leading to inverted spinel-like structures (Co_2AlO_4 or $CoAl_2O_4$). In line with the discussion on alteration of γ-alumina in aqueous media, the peak at 650°C may be assigned to surface Co–Al mixed oxide phase which is formed after impregnation as amorphous phase and crystallises *in situ* during the course of the TPR analysis. The crystallisation of the Co–Al mixed oxide phase on calcination can also be inferred by the observed progressive sharpening of γ-peaks with increasing calcination temperature. This inference agrees with similar conclusion by Ji et al., (2000) who proposed that Co_3O_4 phase on Co/Al_2O_3 prepared by impregnation method is interfaced with other cobalt surface phase. We proposed that the cobalt phase in the third peak (γ-peak) of the calcined alumina supported catalysts is likely to be Co_2AlO_4 since the peak temperature is ~ 520°C which near to 480°C. But this Co_2AlO_4 phase could not be identified by XRD analysis due to very similar lattice parameters of the phases namely Co_3O_4, Co_2AlO_4 and $CoAl_2O_4$ (Walsh et al., 2007).

Conclusion

H-TPR profiles of unsupported cobalt catalysts calcined at different temperatures are used as reference for TPR profiles of the supported catalysts. The amount of residual nitrate decreases with increasing calcination temperature. Reduction Co_3O_4 to Co occurs in two stages: $Co_3O_4 \rightarrow CoO \rightarrow Co$ at temperature ranges of 200 to 400°C and 220 to 330°C for unsupported and supported catalysts, respectively. The two reduction steps take place within same temperature region with single peak maximum in the supported catalysts. Calcination temperature does not have significant effect on reducibility of alumina supported Co_3O_4, but 250°C is considered a reasonable compromise between achieving high nitrate removal and Co_3O_4 dispersion. The result of this study is not consistent with the interpretation of TPR profile of phase Co_3O_4 on alumina support in terms of a two stage reduction process with peak temperatures at 200 to 400°C and 400 to 800°C, respectively. We suggest that consideration of the tendency of dissolution of alumina during the impregnation of metal salt will be beneficial toward achieving higher reducibility of Co_3O_4 in the design of cobalt based Fischer-Tropsch catalysts.

Conflict of interests

The authors have not declared any conflict of interest.

ACKNOWLEDGEMENTS

James is grateful to TWAS (Triestle, Italy) and CSIR (India) for postgraduate fellowship.

REFERENCES

Ay AN, Zümreoglu-Karan B, Mafra L (2009). A Simple Mechanochemical Route to Layered Double Hydroxides: Synthesis of Hydrotalcite-Like Mg-Al-NO_3-LDH by Manual Grinding in a Mortar. Zeitschrift für anorganische und allgemeine Chemie 635(9-10):1470-1475.

Belambe AR, Oukaci R, Goodwin JG (1997). Effect of Pretreatment on the Activity of a Ru-Promoted Co/Al_2O_3 Fischer-Trpsch Catalyst. J. Catal. 166:8-15.

Borg Ø, Blekkan EA, Eri S, Akporiaye D, Vigerust B, Rytter E, Holmen A (2007). Effect of calcination atmosphere and temperature on γ-Al_2O_3 supported cobalt Fischer-Tropsch catalysts. Topics Catal. 45(August):39-43.

Carriera X, Marceaua E, Lamberta J-F, Chea M (2007). Transformations of γ-alumina in aqueous suspensions. J. Colloid Interface Sci. 308(2):429-437.

Chen Y, Wu D, Yeh C (2003). Oxidation of carbon monoxide over nanoparticles of cobalt oxides. Rev. Adv. Mater. Sci. pp. 41-46.

Chu W, Chernavskii PA, Gengembre L, Pankina GA, Fongarland P, Khodakov AY (2007). Cobalt species in promoted cobalt alumina-supported Fischer–Tropsch catalysts. J. Catal. 252(2):215-230.

Dry ME (2002). The Fischer-Tropsch process: 1950-2000. Catal. Today 71(3-4):227-241.

Ehrhardt C, Gjikaj M, Brockner W (2005). Thermal decomposition of cobalt nitrato compounds: Preparation of anhydrous cobalt(II)nitrate and its characterisation by Infrared and Raman spectra. Thermochim. Acta 432(1):36-40.

Girardon JS, Quinet E, Griboval-Constant A, Chernavskii PA, Gengembre L, Khodakov AY (2007). Cobalt dispersion, reducibility, and surface sites in promoted silica-supported Fischer-Tropsch catalysts. J. Catal. 248(2):143-157.

Iglesia E (1997). Design, synthesis, and use of cobalt-based Fischer-Tropsch synthesis catalysts. Appl. Catal. A Gen. 161:59-78.

Jacobs G, Patterson PM, Zhang Y, Das T, Li J, Davis BH (2002). Fischer–Tropsch synthesis: deactivation of noble metal-promoted Co/Al_2O_3 catalysts. Appl Catal. A Gen. 233:215-226.

Jacobs G, Ji Y, Davis B, Cronauer DC, Kropf AJ, Marshall CL (2007). Fischer–Tropsch synthesis: Temperature programmed EXAFS/XANES investigation of the influence of support type, cobalt loading, and noble metal promoter addition to the reduction behaviour of cobalt oxide particles. Appl. Catal. A. Gen. 333(2):177-191.

Ji L, Lin J, Zeng HC (2000). Metal-support interactions in Co/Al_2O_3 catalysts: A comparative study on reactivity of support. J. Phys. Chem. B. 104:1783-1790.

Kagan DN, Lapidus AL, Shpil'rain EE (2008). Process for the production of synthetic liquid fuel based on the conversion of solid fossil fuels and natural gas. Khimiya Tverdogo Topliva (Moscow, Russian Federation), 42(Copyright (C) 2012 American Chemical Society (ACS). All Rights Reserved.). pp. 6-8.

Khassin AA, Yurieva TM, Kustova GN, Itenberg ShI, Demeshkina MP, Krieger TA, Plyasova LM, Chermashentseva GK, Parmon VN(2001). Cobalt-aluminum co-precipitated catalysts and their performance in the Fischer-Tropsch synthesis. J. Mol. Catal. A: Chem. 168(1-2):193-207.

Khodakov AY (2009). Enhancing cobalt dispersion in supported Fischer-Tropsch catalysts via controlled decomposition of cobalt precursors. Brazilian J. Phys. 39(1):171-175.

Pe JR, Mul G, Kapteijn F, Moulijn JA (2001). *In situ* investigation of the thermal decomposition of Co ± Al hydrotalcite in different atmospheres. J. Mater. Chem. 11:821-830.

Perego C (2007). Development of a Fischer-Tropsch catalyst: From laboratory to commercial scale demonstration. Rendiconti Lincei 18(4):305-317.

Potoczna-Petru D, Kępiński L (2001). Reduction study of Co_3O_4 model catalyst by electron microscopy. Catal. Lett. 73(1):41-46.

Schulz H (1999). Short history and present trends of Fischer–Tropsch synthesis. Appl. Catal. A: Gen. 186(1-2):3-12.

Schulz H (2003). Spatial constraints and frustrated reactions in Fischher-Tropsch synthesis. Catal. Today 84(1-2):67-70.
Sirijaruphan A, Horváth A, Goodwin Jr. JG, Oukaci R (2003). Cobalt aluminate formation in alumina-supported cobalt catalysts: Effects of cobalt reduction state and water vapor. Catal. Lett. 91(1):89-94.
Tang C-W, Wang C-B, Chien S-H (2008). Characterization of cobalt oxides studied by FT-IR, Raman, TPR and TG-MS. Thermochim. Acta 473(1-2):68-73.
Trueba M, Trasatti SP (2005). γ-Alumina as a Support for Catalysts: A Review of Fundamental Aspects. Eur. J. Inorg. Chem. 17:3393-3403.
Walsh A, Wei SH, Yan Y, Al-Jassim MM, Turner JA, Woodhouse M, Parkinson BA (2007). Structural, magnetic, and electronic properties of the Co-Fe-Al oxide spinel system: Density-functional theory calculations. Phys. Rev. B. 76(16):165119.
Wang CB, Lin HK, Tang CW (2004). Thermal characterization and microstructure change of cobalt oxides. Catal. Lett. 94(1-2):69-74.
Yuvaraj S, Fan-Yuan L, Tsong-Huei C, Chuin-Tih Y (2003). Thermal decomposition of metal nitrates in air and hydrogen environments. J. Phys. Chem. B. 107(4):1044-1047.
Zhang J, Chen J, Li YW, Sun Y (2002). Recent Technological Developments in Cobalt Catalysts for Fischer-Tropsch Synthesis. J. Nat. Gas Chem. 11(3-4):99-108.